PORTLAND
PRESS

Commentary

A home run for human NaCT/SLC13A5/INDY: cryo-EM structure and homology model to predict transport mechanisms, inhibitor interactions and mutational defects

Valeria Jaramillo-Martinez[1], Vadivel Ganapathy[2] and Ina L. Urbatsch[2]

[1]Department of Pharmacology and Neuroscience, Texas Tech University Health Sciences Center, Lubbock, TX, U.S.A.; [2]Department of Cell Biology and Biochemistry, Texas Tech University Health Sciences Center, Lubbock, TX, U.S.A.

Correspondence: Ina L. Urbatsch (ina.urbatsch@ttuhsc.edu)

OPEN ACCESS

NaCT (SLC13A5) is a Na^+-coupled transporter for citrate, which is expressed in the liver, brain, testes, and bone. It is the mammalian homolog of *Drosophila* INDY, a cation-independent transporter for citrate, whose partial loss extends lifespan in the organism. In humans, loss-of-function mutations in NaCT cause a disease with severe neurological dysfunction, characterized by neonatal epilepsy and delayed brain development. In contrast with humans, deletion of NaCT in mice results in a beneficial metabolic phenotype with protection against diet-induced obesity and metabolic syndrome; the brain dysfunction is not readily noticeable. The disease-causing mutations are located in different regions of human NaCT protein, suggesting that different mutations might have different mechanisms for the loss of function. The beneficial effects of NaCT loss in the liver versus the detrimental effects of NaCT loss in the brain provide an opportunity to design high-affinity inhibitors for the transporter that do not cross the blood-brain barrier so that only the beneficial effects could be harnessed. To realize these goals, we need a detailed knowledge of the 3D structure of human NaCT. The recent report by Sauer et al. in Nature describing the cryo-EM structure of human NaCT represents such a milestone, paving the way for a better understanding of the structure-function relationship for this interesting and clinically important transporter.

INDY (I'm Not Dead Yet) is a transport protein whose partial loss of function confers a lifespan advantage in *Drosophila* [1]. The mammalian homolog of INDY is the Na^+-coupled citrate transporter NaCT (also known as SLC13A5) [2–5]. Both INDY and NaCT accept citrate, a key metabolite, as their preferred substrate [2–7]. Just as a caloric-restriction diet increases longevity and delays age-associated disorders, the loss of INDY in *Drosophila* or deletion of *Slc13a5* in mice elicit similar survival and lifespan benefits [1,8]. Notwithstanding this significant resemblance in the biological functions of INDY and NaCT, loss of the transporter in mammals produces a detrimental neurological dysfunction, though evident much more readily in humans than in mice [7–10]. In humans, loss of function mutations cause a recessive neurological disease known as Early Infantile Epileptic Encephalopathy-25 (EIEE-25) [9–12]. This disease is characterized by neonatal epilepsy, delayed brain development and language skills, defective bone mineralization, and abnormal tooth development and enamelization. In contrast, *Slc13a5*-null mice show minimal evidence of neurological dysfunction [13], but a robust beneficial metabolic phenotype relating to the loss of function of the transporter in the liver [8]; the beneficial features include resistance to diet-induced obesity, protection against diabetes and insulin resistance, and other clinical features of metabolic syndrome [8]. Considering the vastly

differing consequences of NaCT deficiency in the brain versus the periphery, we recently hypothesized that it could be feasible to preferentially harness the beneficial effects of NaCT deficiency by developing inhibitors that only block the function of the transporter in the liver without having access to the brain [11]. This would avoid the detrimental neurological phenotype associated with the loss of function in the brain. Several high-affinity inhibitors of NaCT have already been identified, and kinetic studies have unveiled significant differences among these inhibitors in terms of their interaction with the transporter [14–19]. In EIEE-25 patients with mutations in NaCT, the detrimental neurological consequences in the brain associated with the loss of function of NaCT take the precedence over any potential metabolic benefits. Approximately 40 disease-causing mutations, spread over different loci of the transporter protein, have been identified [20]. The mechanisms underlying the functional loss of the transporter vary among these mutations. Some missense mutants exhibit normal protein production and trafficking to the plasma membrane but have no transport function, whereas others suffer from protein expression, folding and trafficking defects, and thus the mutant proteins fail to reach the plasma membrane [21–24]. To understand full well the consequences of the different mutations at the molecular level, we require a detailed knowledge of the structure of the protein and the relevance of the disease-causing mutations to protein folding and function. The same applies to the rational development of high-affinity inhibitors for identifying those that do not permeate the blood-brain barrier. As such, availability of information on the structure of NaCT is of paramount importance in several key areas pertaining to the biology and pharmacology of this interesting transporter.

Until recently, the only way to gain insights into the structural architecture and structure-function relations of NaCT was through homology modeling of a closely related transporter protein of known structure. For most modeling studies of NaCT thus far, *Vibrio cholerae* INDY (VcINDY) served as the template [17,21–23,25–27], even though the two proteins share only ~30% sequence identity and their transport functions are vastly different. In truth, the term 'INDY' should have never been applied to VcINDY because it is actually a dicarboxylate (succinate and fumarate) transporter, in contrast with *Drosophila* INDY and mammalian NaCT, which are tricarboxylate (citrate) transporters. As such, VcINDY is more closely related to other members of the divalent anion/Na$^+$ symporter (DASS) subfamily, to mammalian SLC13A1 and SLC13A3, which are Na$^+$-coupled dicarboxylate transporters. Understandably, these two transporters are never referred to as INDY. Notwithstanding this marked functional difference, the VcINDY was the closest relative for which a crystal structure was available [26,27]. This has changed recently with the elucidation of the cryogenic electron microscopy (cryo-EM) structure of human NaCT by Sauer et al. (PDB: 7JSK) [28]. With this fundamental advancement, we now have an important piece of the puzzle. However, until we can obtain more structures of NaCT in different conformations and with a variety of bound inhibitors and modulators, we may rely on homology modeling, docking and molecular dynamic (MD) simulations to gain a more complete understanding of the molecular transport mechanism. Our recent full-length 3D homology model of human NaCT [10] (Protein Model Database ID PM0083164) is astonishingly similar to the new NaCT cryo-EM structure, with a Cα backbone root-mean-square deviation (RMSD) of 2 Å for 87% of the amino acids (Figure 1A). However, as is common in homology models, the sidechains of some residues are in different orientations. Our model was built using Robetta, a full-chain protein structure prediction server [29,30], based on the structures of VcINDY (PDB IDs: 4f35 [26], 5uld [27]) as well as an ion transporter of the AbgT family, YdaH from *Alcanivorax borkumensis* (PDB: 4R0C) that share similar α-helical domain architecture [31,32]. The model includes ~100 amino acids of the large second intracellular loop whose structure was not resolved in the recently reported cryo-EM structure. This loop doesn't contain any disease-causing mutation. The homology model assigned mostly α-helical structure that may help stabilize the transporter in the membrane.

The NaCT cryo-EM structure shows a homodimer with the citrate-binding site of both protomers accessible to the cytoplasm (arrows) in the 'inward-facing' conformation. Figure 1 shows an overlay of one protomer of our model (colored) onto the cryo-EM structure with one bound citrate molecule (green sticks) and two Na$^+$ ions (purple spheres). The 11 transmembrane α-helices (TMs) of each protomer form a scaffold domain (blue) that dimerizes with the other protomer (Figure 1B), and a transport domain that harbors the binding sites for Na$^+$ and citrate. The inverted repeat pseudo-symmetry arrangement of TM2–6 and TM7–11 as well as the arrangement of the two helix-turn-helix hairpins, HP$_{in}$ and HP$_{out}$ (brown-orange and red-yellow) that cradle the Na$^+$- and citrate-binding sites, are similar to VcINDY and YdaH. Interestingly, TM5 and TM10, adjacent to the HP$_{in}$ and HP$_{out}$ helices, respectively, are broken in the middle of the lipid bilayer of the membrane, and the connecting loops contribute to the Na$^+$/citrate binding sites. This arrangement of two hairpin loops that insert into the membrane from opposite sides, and the two broken transmembrane helices are common in
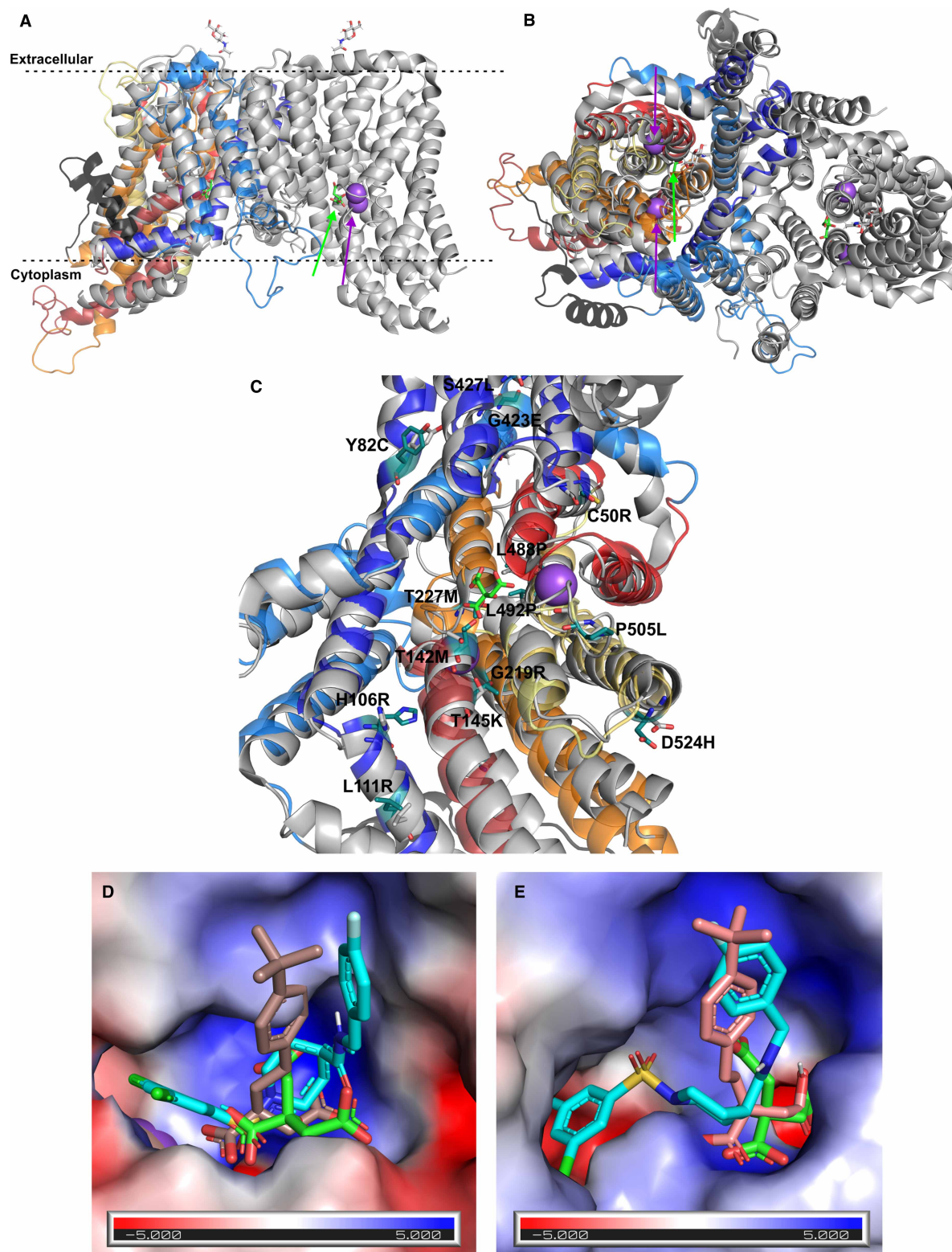
Figure 1. Comparison between the new cryo-EM structure and our full-length homology model of human NaCT.

Part 1 of 2

(**A**) Ribbon diagram of the NaCT cryo-EM structure (gray, PDB: 7JSK) [28]) in the inward-facing conformation is viewed in the membrane plane. The N-terminus resides in the cytoplasm and the C-terminus in the extracellular space. Na$^+$ ions are shown in purple spheres (purple arrow) and citrate in green sticks (green arrow). Our full-length homology model [10] was

Figure 1. Comparison between the new cryo-EM structure and our full-length homology model of human NaCT.

superimposed in the left protomer of the dimer, colored according to helix organization of the scaffold domain (blue and light blue), and transport domain (dark red and red for hairpins, and orange and yellow for interfacial helices, respectively). The half helix H6b in the cryo-EM structure, located between TM6 and TM7, was correctly predicted as a helix by our homology model (black). (**B**) Extracellular view showing the dimer interface, formed by the scaffold domain from each protomer. Na^+ ions are shown in purple spheres (purple arrow) and citrate in green sticks (green arrow). (**C**) Localization of disease-causing mutations in the cryo-EM structure (gray sticks) and in the homology model (teal sticks). (**D**) An overlay of citrate (green sticks), and inhibitors PF2 (pink sticks) and BI0 (cyan sticks) bound to the citrate-binding surface in the cryo-EM structure, colored according to electrostatic surface potential. (**E**) An overlay of the citrate, PF2 and BI0 bound to our homology model; the electrostatic surface potential ranges from bright blue (positive) to red (negative).

proteins that use the elevator type mechanism to transport substrates across the membrane using preexisting gradients of ions (e.g. Na^+) as the driving force [26,27,31–34]. In these elevator-type transporters, typically the scaffold domains of the protomers associate back-to-back and anchor the protein in the membrane, while the transport domains move to expose the substrate-binding site from the extracellular to the cytoplasmic side of the membrane, and back. It has to be noted that the 3D structure of a member of the DASS family in an outward conformation has been solved so far only for the *Lactobacillus acidophilus* transporter LaINDY [35]. Recent MD simulations based on the LaINDY structure elegantly proposed that the transport domains of both protomers move simultaneously to transport citrate and Na^+ from the extracellular to the intracellular site of the membrane in a synchronized fashion [35]. In contrast, the 3D-structure of another bacterial Na^+-dependent citrate transporter, KpCitS, shows dimers either with one protomer in the inward-facing and one in the outward-facing conformation (asymmetric dimer), or with both protomers outward-facing (symmetric dimer), suggesting that the transport domains may move independently [36]. Based on biochemical analyses of VcINDY [37], we proposed an asymmetric outward-facing conformation for human NaCT [10]. However, global elevator movements may vary widely between different proteins and protein families, and more biophysical studies will be needed to clarify whether the two NaCT protomers may function cooperatively or independently.

The new cryo-EM structure of human NaCT, together with homology models of different conformations, as well as MD simulations of substrate transport open up new avenues to predict and probe the underlying molecular defects of disease-causing mutations in EIEE-25, an important step towards designing targeted treatment. Limited cell biological and biochemical analyses are available only for a few mutants, largely due to the lack of highly selective antibodies that are capable of recognizing the human NaCT protein in immunofluorescence and/or western blot studies. In principle, mutations can be classified as functional missense mutations (Class I) that abolish or decrease Na^+-coupled citrate transport, protein-folding missense mutations (Class II) that affect protein expression, folding and stability, and may lead to defective trafficking to the cell surface, and protein synthesis and nonsense mutations (Class III) that affect translation of the gene. Class I mutations are located in the substrate-binding site and are directly involved in binding of citrate and Na^+ (subclass IA); amino acid substitutions at these positions will weaken the protein-substrate binding affinity (T142M, T227M and P505L, Figure 1C) and diminish transport. The Class I mutations are also located at the interface of the scaffold and transport domains and may interfere with the proposed elevator-type transport mechanism (subclass IB: C50R, H106R, L111R and G417E). The latter have been described as 'conformational defect mutations' by Sauer et al. [28]. Patients with these mutations could benefit from pharmacological strategies capable of potentiating the transport function. The Class II mutations may cause local misfolding of the protein that is recognized by the quality control machinery in the endoplasmic reticulum (ER) and targeted for premature degradation. Such mutant proteins do not exit the ER, and do not reach the Golgi apparatus for maturation and post-translational modification, thus resulting in trafficking defects and lack of protein at the cell surface. According to their location in the structure (Figure 1C), this class may be subdivided into subclass IIA (P68Q, Y82C, and G423E; mutations located in the scaffold domain) and subclass IIB (T145K, G130D, P487L, L488P, and L492P; mutations located in the transport domain). For these folding and trafficking mutations, small-molecule correctors may be developed that promote folding and rescue from the ER quality control and facilitate proper maturation and trafficking to the plasma membrane. This approach has been very successful for the treatment of other genetic disorders such as cystic fibrosis [38,39]. Lastly, the Class III mutations comprise nonsense mutations or stop codons, splicing mutations and promotor variants that interfere with protein

synthesis, and may require gene editing or gene replacement strategies. There is a very good agreement between the classifications of the disease-causing mutations based either on the new cryo-EM structure of human NaCT [28] or on our homology-based model [10]. One notable exception however is G219R, the most predominant mutation in EIEE-25 patients. We proposed that the primary defect with this mutation is related to protein folding because the bulky, positively charged arginine likely disrupts α-helical structure and helix packing of TM5a. In addition, amino acid residues of this helix contribute to the citrate-binding site, and thus disruption of this helix may also weaken substrate binding and transport. For this mutation, a combination of folding correctors and a transport potentiator might be an effective therapeutic option.

High-affinity inhibitors have been developed for NaCT, with the goal to selectively inhibit the transporter in the liver and provide new treatment options for obesity and diabetes [14–19]. The recent report by Sauer et al. [28] is the first to solve the cryo-EM structure of NaCT with a selective inhibitor PF-06649298 (PF2) bound in close proximity to the citrate-binding site in the inward-facing conformation. Figure 1D shows PF2 (pink sticks) interacting with the same residues as citrate, which is expected considering the structural similarity between PF2 and citrate. Both Na^+-binding sites are occupied with Na^+ in the PF2-bound structure, suggesting that Na^+ might be required for the binding of PF2. PF2 interacts with the side chain of the two SNT motifs and T508 residues [28]. We recently characterized a new, highly potent inhibitor, named BI01383298 (BI0), that inhibits human NaCT with IC_{50} values in the nM range [14]. Docking studies using our model suggested BI0 also binds to the same binding pocket as citrate, albeit its chemical structure is quite different (Figure 1E). Collectively, these data suggest that the highly positively charged surface of the citrate-binding pocket may be a common site for inhibitor binding, and presents a good target for *in silico* screening for highly potent, more diverse inhibitors with properties favorable to inhibit liver NaCT and not to cross the blood-brain barrier.

In conclusion, the recent report on the cryo-EM structure of human NaCT undoubtedly represents a milestone and is a home run, giving a clear path to better understand the structure-function relationship for this interesting and clinically relevant transporter. This will definitely facilitate the design of targeted treatment strategies for EIEE-25 and discovery of new inhibitors of NaCT to selectively modulate hepatic metabolism for the management of diet-induced obesity, insulin resistance, diabetes and metabolic syndrome. Indeed, knowledge gained from the new NaCT structure will certainly integrate future homology modeling and docking/MD simulations to gain further insights into the transport mechanism, interactions of different inhibitors, and the impact of various disease-causing mutations.

Competing Interests
The authors declare that there are no competing interests associated with the manuscript.

Funding

Open Access
Open access for this article was enabled by the participation of the Texas Tech University Health Sciences Center in an all-inclusive *Read & Publish* pilot with Portland Press and the Biochemical Society under a transformative agreement with EBSCO.

Author Contribution
V.J-M. prepared the figure and wrote the initial draft of the manuscript. V.G. and I.L.U. edited and finalized the manuscript.

Abbreviations
cryo-EM, cyrogenic electron microscopy; EIEE-25, early infantile epileptic encephalopathy-25; HP, helix-turn-helix hairpin; INDY, I'm Not Dead Yet; MD, molecular dynamics; NaCT, Na^+-coupled citrate transporter; SLC13A5, solute carrier family 13A, member 5; TM, transmembrane domain.

References
1   Rogina, B., Reenan, R.A., Nilsen, S.P. and Helfand, S.L. (2000) Extended life-span conferred by cotransporter gene mutations in *Drosophila. Science*
290, 2137–2140 https://doi.org/10.1126/science.290.5499.2137

2   Gopal, E., Babu, E., Ramachandran, S., Bhutia, Y.D., Prasad, P.D. and Ganapathy, V. (2015) Species-specific influence of lithium on the activity of SLC13A5 (NaCT): lithium-induced activation is specific for the transporter in primates. *J. Pharmacol. Exp. Ther.* **353**, 17–26 https://doi.org/10.1124/jpet.114.221523

3   Inoue, K., Fei, Y.J., Zhuang, L., Gopal, E., Miyauchi, S. and Ganapathy, V. (2004) Functional features and genomic organization of mouse NaCT, a sodium-coupled transporter for tricarboxylic acid cycle intermediates. *Biochem. J.* **378**, 949–957 https://doi.org/10.1042/bj20031261

4   Inoue, K., Zhuang, L. and Ganapathy, V. (2002) Human Na$^+$-coupled citrate transporter: primary structure, genomic organization, and transport function. *Biochem. Biophys. Res. Commun.* **299**, 465–471 https://doi.org/10.1016/S0006-291X(02)02669-4

5   Inoue, K., Zhuang, L., Maddox, D.M., Smith, S.B. and Ganapathy, V. (2002) Structure, function, and expression pattern of a novel sodium-coupled citrate transporter (NaCT) cloned from mammalian brain. *J. Biol. Chem.* **277**, 39469–39476 https://doi.org/10.1074/jbc.M207072200

6   Inoue, K., Fei, Y.J., Huang, W., Zhuang, L., Chen, Z. and Ganapathy, V. (2002) Functional identity of *Drosophila melanogaster* Indy as a cation-independent, electroneutral transporter for tricarboxylic acid-cycle intermediates. *Biochem. J.* **367**, 313–319 https://doi.org/10.1042/bj20021132

7   Knauf, F., Mohebbi, N., Teichert, C., Herold, D., Rogina, B., Helfand, S. et al. (2006) The life-extending gene Indy encodes an exchanger for Krebs-cycle intermediates. *Biochem. J.* **397**, 25–29 https://doi.org/10.1042/BJ20060409

8   Birkenfeld, A.L., Lee, H.-Y., Guebre-Egziabher, F., Alves, T.C., Jurczak, M.J., Jornayvaz, F.R. et al. (2011) Deletion of the mammalian INDY homolog mimics aspects of dietary restriction and protects against adiposity and insulin resistance in mice. *Cell. Metab.* **14**, 184–195 https://doi.org/10.1016/j.cmet.2011.06.009

9   Bhutia, Y.D., Kopel, J.J., Lawrence, J.J., Neugebauer, V. and Ganapathy, V. (2017) Plasma membrane Na$^+$-coupled citrate transporter (SLC13A5) and neonatal epileptic encephalopathy. *Molecules* **22**, 1–15 https://doi.org/10.3390/molecules22030378

10   Jaramillo-Martinez, V., Urbatsch, I.L. and Ganapathy, V. (2021) Functional distinction between human and mouse sodium-coupled citrate transporters and its biologic significance: an attempt for structural basis using a homology modeling approach. *Chem. Rev.* **121**, 5359–5377 https://doi.org/10.1021/acs.chemrev.0c00529

11   Kopel, J.J., Bhutia, Y.D., Sivaprakasam, S. and Ganapathy, V. (2021) Consequences of NaCT/SLC13A5/mINDY deficiency: good versus evil, separated only by the blood–brain barrier. *Biochem. J.* **478**, 463–486 https://doi.org/10.1042/BCJ20200877

12   Willmes, D.M., Kurzbach, A., Henke, C., Schumann, T., Zahn, G., Heifetz, A. et al. (2018) The longevity gene INDY (I'm Not Dead Yet) in metabolic control: Potential as pharmacological target. *Pharmacol. Ther.* **185**, 1–11 https://doi.org/10.1016/j.pharmthera.2017.10.003

13   Henke, C., Töllner, K., van Dijk, R.M., Miljanovic, N., Cordes, T., Twele, F. et al. (2020) Disruption of the sodium-dependent citrate transporter SLC13A5 in mice causes alterations in brain citrate levels and neuronal network excitability in the hippocampus. *Neurobiol. Dis.* **143**, 105018 https://doi.org/10.1016/j.nbd.2020.105018

14   Higuchi, K., Kopel, J.J., Sivaprakasam, S., Jaramillo-Martinez, V., Sutton, R.B., Urbatsch, I.L. et al. (2020) Functional analysis of a species-specific inhibitor selective for human Na$^+$-coupled citrate transporter (NaCT/SLC13A5/mINDY). *Biochem. J.* **477**, 4149–4165 https://doi.org/10.1042/BCJ20200592

15   Huard, K., Brown, J., Jones, J.C., Cabral, S., Futatsugi, K., Gorgoglione, M. et al. (2015) Discovery and characterization of novel inhibitors of the sodium-coupled citrate transporter (NaCT or SLC13A5). *Sci. Rep.* **5**, 17391 https://doi.org/10.1038/srep17391

16   Huard, K., Gosset, J.R., Montgomery, J.I., Gilbert, A., Hayward, M.M., Magee, T.V. et al. (2016) Optimization of a dicarboxylic series for in vivo inhibition of citrate transport by the solute carrier 13 (SLC13) family. *J. Med. Chem.* **59**, 1165–1175 https://doi.org/10.1021/acs.jmedchem.5b01752

17   Pajor, A.M., de Oliveira, C.A., Song, K., Huard, K., Shanmugasundaram, V. and Erion, D.M. (2016) Molecular basis for inhibition of the Na$^+$/citrate transporter NaCT (SLC13A5) by dicarboxylate inhibitors. *Mol. Pharmacol.* **90**, 755–765 https://doi.org/10.1124/mol.116.105049

18   Rives, M.L., Shaw, M., Zhu, B., Hinke, S.A. and Wickenden, A.D. (2016) State-dependent allosteric inhibition of the human SLC13A5 citrate transporter by hydroxysuccinic acids, PF-06649298 and PF-06761281. *Mol. Pharmacol.* **90**, 766–774 https://doi.org/10.1124/mol.116.106575

19   Sun, J., Aluvila, S., Kotaria, R., Mayor, J.A., Walters, D.E. and Kaplan, R.S. (2010) Mitochondrial and plasma membrane citrate transporters: discovery of selective inhibitors and application to structure/function analysis. *Mol. Cell. Pharmacol.* **2**, 101–110 PMID:20686672

20   TessResearchFoundation. Full list of pathogenic SLC13A5 mutations. https://tessresearch.org/

21   Hardies, K., De Kovel, C.G., Weckhuysen, S., Asselbergh, B., Geuens, T., Deconinck, T. et al. (2015) Recessive mutations in SLC13A5 result in a loss of citrate transport and cause neonatal epilepsy, developmental delay and teeth hypoplasia. *Brain* **138**, 3238–3250 https://doi.org/10.1093/brain/awv263

22   Klotz, J., Porter, B.E., Colas, C., Schlessinger, A. and Pajor, A.M. (2016) Mutations in the Na$^+$/citrate cotransporter NaCT (SLC13A5) in pediatric patients with epilepsy and developmental delay. *Mol. Med.* **22**, 310–321 https://doi.org/10.2119/molmed.2016.00077

23   Selch, S., Chafai, A., Sticht, H., Birkenfeld, A.L., Fromm, M.F. and Konig, J. (2018) Analysis of naturally occurring mutations in the human uptake transporter NaCT important for bone and brain development and energy metabolism. *Sci. Rep.* **8**, 11330 https://doi.org/10.1038/s41598-018-29547-8

24   Thevenon, J., Milh, M., Feillet, F., St-Onge, J., Duffourd, Y., Jugé, C. et al. (2014) Mutations in SLC13A5 cause autosomal-recessive epileptic encephalopathy with seizure onset in the first days of life. *Am. J. Hum. Genet.* **95**, 113–120 https://doi.org/10.1016/j.ajhg.2014.06.006

25   Khamaysi, A., Aharon, S., Eini-Rider, H. and Ohana, E. (2020) A dynamic anchor domain in SLC13 transporters controls metabolite transport. *J. Biol. Chem.* **295**, 8155–8163 https://doi.org/10.1074/jbc.RA119.010911

26   Mancusso, R., Gregorio, G.G., Liu, Q. and Wang, D.N. (2012) Structure and mechanism of a bacterial sodium-dependent dicarboxylate transporter. *Nature* **491**, 622–626 https://doi.org/10.1038/nature11542

27   Nie, R., Stark, S., Symersky, J., Kaplan, R.S. and Lu, M. (2017) Structure and function of the divalent anion/Na$^+$ symporter from *Vibrio cholerae* and a humanized variant. *Nat. Commun.* **8**, 15009 https://doi.org/10.1038/ncomms15009

28   Sauer, D.B., Song, J., Wang, B., Hilton, J.K., Karpowich, N.K., Mindell, J.A. et al. (2021) Structure and inhibition mechanism of the human citrate transporter NaCT. *Nature* **591**, 157–161 https://doi.org/10.1038/s41586-021-03230-x

29   Raman, S., Vernon, R., Thompson, J., Tyka, M., Sadreyev, R., Pei, J. et al. (2009) Structure prediction for CASP8 with all-atom refinement using Rosetta. *Proteins* **77**, 89–99 https://doi.org/10.1002/prot.22540

30   Song, Y., DiMaio, F., Wang, R.Y., Kim, D., Miles, C., Brunette, T. et al. (2013) High-resolution comparative modeling with RosettaCM. *Structure* **21**, 1735–1742 https://doi.org/10.1016/j.str.2013.08.005

31   Bolla, J.R., Su, C.C., Delmar, J.A., Radhakrishnan, A., Kumar, N., Chou, T.H. et al. (2015) Crystal structure of the *Alcanivorax borkumensis* YdaH transporter reveals an unusual topology. *Nat. Commun.* **6**, 6874 https://doi.org/10.1038/ncomms7874

32 Su, C.-C., Bolla, J.R., Kumar, N., Radhakrishnan, A., Long, F., Delmar, J.A. et al. (2015) Structure and function of *Neisseria gonorrhoeae* MtrF illuminates a class of antimetabolite efflux pumps. *Cell Rep.* **11**, 61–70 https://doi.org/10.1016/j.celrep.2015.03.003

33 Drew, D. and Boudker, O. (2016) Shared molecular mechanisms of membrane transporters. *Annu. Rev. Biochem.* **85**, 543–572 https://doi.org/10.1146/annurev-biochem-060815-014520

34 Garaeva, A.A. and Slotboom, D.J. (2020) Elevator-type mechanisms of membrane transport. *Biochem. Soc. Trans.* **48**, 1227–1241 https://doi.org/10.1042/BST20200290

35 Sauer, D.B., Trebesch, N., Marden, J.J., Cocco, N., Song, J., Koide, A. et al. (2020) Structural basis for the reaction cycle of DASS dicarboxylate transporters. *eLife* **9**, e61350 https://doi.org/10.7554/eLife.61350

36 Kim, J.W., Kim, S., Kim, S., Lee, H., Lee, J.O. and Jin, M.S. (2017) Structural insights into the elevator-like mechanism of the sodium/citrate symporter CitS. *Sci. Rep.* **7**, 2548 https://doi.org/10.1038/s41598-017-02794-x

37 Mulligan, C., Fenollar-Ferrer, C., Fitzgerald, G.A., Vergara-Jaque, A., Kaufmann, D., Li, Y. et al. (2016) The bacterial dicarboxylate transporter VcINDY uses a two-domain elevator-type mechanism. *Nat. Struct. Mol. Biol.* **23**, 256–263 https://doi.org/10.1038/nsmb.3166

38 Middleton, P.G., Mall, M.A., Dřevínek, P., Lands, L.C., McKone, E.F., Polineni, D. et al. (2019) Elexacaftor–tezacaftor–ivacaftor for cystic fibrosis with a single Phe508del allele. *N. Engl. J. Med.* **381**, 1809–1819 https://doi.org/10.1056/NEJMoa1908639

39 Quon, B.S. and Rowe, S.M. (2016) New and emerging targeted therapies for cystic fibrosis. *BMJ* **352**, i859 https://doi.org/10.1136/bmj.i859